Solvent-Induced Cluster-to-Cluster Transformation of Homoleptic Gold(I) Thiolates: between Catenane and Ring-in-Ring Structures

Guang-Tao Xu,[+] Liang-Liang Wu,[+] Xiao-Yong Chang, Tim Wai Hung Ang, Wai-Yeung Wong, Jie-Sheng Huang,* and Chi-Ming Che*

Abstract: *Supramolecular ensembles adopting ring-in-ring structures are less developed compared with catenanes featuring interlocked rings. While catenanes with inter-ring closed-shell metallophilic interactions, such as d^{10}-d^{10} Au(I)-Au(I), have been well-documented, the ring-in-ring complexes featuring such metallophilic interactions remain underdeveloped. Herein is described an unprecedented ring-in-ring structure of Au(I)-thiolate Au_{12} cluster formed by recrystallization of a Au(I)-thiolate Au_{10} [2]catenane from alkane solvents such as hexane, with use of a bulky dibutyl-fluorene-2-thiolate ligand. The ring-in-ring Au(I)-thiolate Au_{12} cluster features inter-ring Au(I)-Au(I) interactions and underwent cluster core change to form the thermodynamically more stable Au_{10} [2]catenane structure upon dissolving in, or recrystallization from, other solvents such as CH_2Cl_2, $CHCl_3$, and CH_2Cl_2/MeCN. Both the ring-in-ring and [2]catenane structures have been characterized by NMR spectroscopy, ESI-MS spectrometry, elemental analysis, and X-ray crystal structure determination. The cluster-to-cluster transformation process in solution was monitored by ^{1}H NMR and ESI-MS measurements. Density functional theory (DFT) calculations were performed to provide insight into the mechanism of the 'ring-in-ring ↔ [2]catenane' interconversions, which could be rationalized by considering various interactions including ligand-ligand and metal-ligand dispersive interaction as well as metallophilic interaction.*

Introduction

Complexes composed of two or multiple rings interlocked or held together by noncovalent interactions have intrigued supramolecular chemists for decades not only for their unique and fascinating structures, but also for their potential applications in catalysis and molecular machines.[1] In the system comprising two rings, [2]catenanes featuring interlocked rings (Figure 1a) have been well explored,[2] whereas the ring-in-ring complexes, in which one macrocycle threads through another with their mean planes roughly perpendicular to each other (Figure 1b),[3] or two different-sized macrocycles are essentially parallel/co-planar[4a,b,d,f,g] or adopt other orientations[4c,e,h,5] forming Russian dolls,[4b,e,g,h] gyroscane,[4c] or a ring-in-ring rotaxane,[5] remain a challenging goal in noncovalent synthesis.[6] Ring-in-ring complexes are also key intermediates for the preparation of molecular Borromean rings.[3,7] As up to now, a number of ring-in-ring complexes consisting of organic macrocycles[3,4a-f,h,5] held together by hydrogen bonding (Figure 1c),[3a] donor-acceptor,[3c] or host-guest[3d,4a-f,h,5] interactions have been reported, together with some examples of ring-in-ring metal complexes, in which the two noninterlocked rings were constructed or held together by metal-ligand coordination bonds[7b,d,8,9,10] (such as M–N (M = Cu,[8a] Pd,[9a,c,10a,b] Ru,[7b,d,8b] Ir,[9d] Pt,[9c] Zn[4g]) and M–O (M = Ru,[9b] Ir[9d]), e.g. Figure 1d–f) or held together by π-π stacking (Figure 1d,f)[7h,9] or hydrophobic interactions.[10]

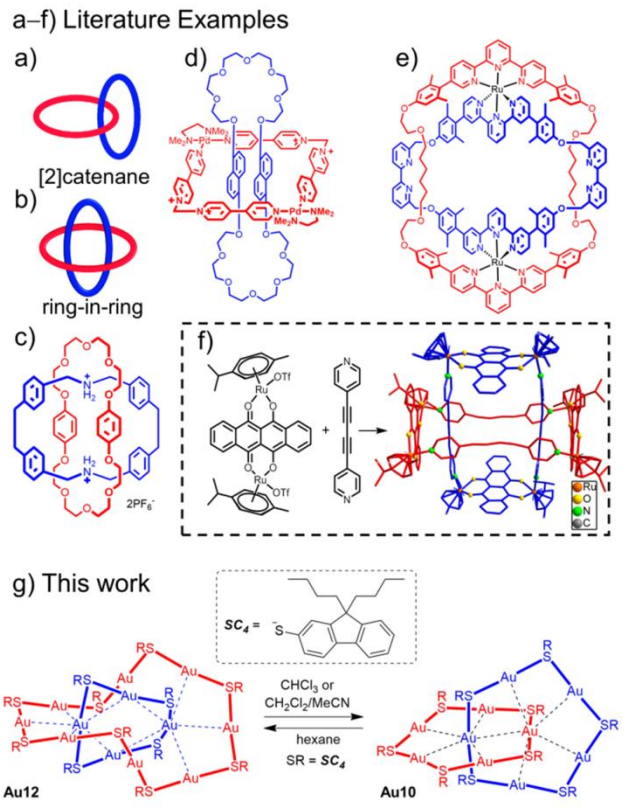

Figure 1. Schematic representation of [2]catenane (a), ring-in-ring structure (b) and literature examples of ring-in-ring structure (c,[3a] d,[9a] e,[8b] and f[9b]) and the Au(I)-thiolate ring-in-ring cluster **Au12** and interconversion between **Au12** and [2]catenane **Au10** reported in this work.

[*] G.-T. Xu, Dr. L.-L. Wu, Dr. X.-Y. Chang, Dr. T. W. H. Ang, Dr. J.-S. Huang, Prof. Dr. C.-M. Che
State Key Laboratory of Synthetic Chemistry, Institute of Molecular Functional Materials, HKU-CAS Joint Laboratory on New Materials, and Department of Chemistry, The University of Hong Kong, Pokfulam Road, Hong Kong SAR (China)
E-mail: cmche@hku.hk
jshuang@hku.hk

Prof. Dr. C.-M. Che
HKU Shenzhen Institute of Research and Innovation, Shenzhen 518053 (China)

Prof. W.-Y. Wong
Department of Applied Biology and Chemical Technology, The Hong Kong Polytechnic University, Hung Hom, Hong Kong SAR (China)

[+] These authors contributed equally to this work.

Supporting information for this article is given via a link at the end of the document.

Closed-shell metallophilic interactions are comparable in strength with a typical hydrogen bond,[11] and have been used in the formation of catenanes, as demonstrated by the [2]catenane structures in, for example, the homoleptic homometallic Au(I)-alkynyl or -thiolate complexes $[Au(C{\equiv}C\textit{t}Bu)]_{12}$,[12] $[Au(C{\equiv}CR)]_{10}$,[13] $[Au(SR)]_n$ (n = 10,[14] 11,[15] 12[14]), heteroleptic Au^I-alkynyl/phosphine complexes,[16] and heterometallic Cu(I)/Ag(I)/Au(I)-alkynyl complexes,[17] and also the [3]catenane structure in Cu(I)-alkynyl complex $[Cu(C{\equiv}C\textit{t}Bu)]_{20}$.[18] The previous works on Au(I)-alkynyl or -thiolate catenanes highlight the role of Au(I)···Au(I) interaction in the assembly of interlocked rings. However, to the best of our knowledge, *the assembly of a ring-in-ring complex in which the noninterlocked rings are held together by closed-shell metallophilic interactions has not been reported.*

Herein, we report the unexpected formation of a homoleptic Au(I)-thiolate cluster, $[Au(\boldsymbol{SC_4})]_{12}$ (**Au12**, Figure 1g), with a novel ring-in-ring structure featuring a $[Au(\boldsymbol{SC_4})]_8$ ring encapsulating another $[Au(\boldsymbol{SC_4})]_4$ ring, stabilized by weak Au(I)···Au(I) interactions and a bulky dibutyl-fluorene-2-thiolate ligand ($\boldsymbol{SC_4}$). Intriguingly, the ring-in-ring cluster **Au12** can be quantitatively transformed to [2]catenane $[Au(\boldsymbol{SC_4})]_{10}$ (**Au10**, Figure 1g) with a pair of interlocked $[Au(\boldsymbol{SC_4})]_5$ rings upon dissolving in $CHCl_3$ or CH_2Cl_2/MeCN, and re-assembled by slow recrystallization of **Au10** from alkane solvents such as hexane. The interconversion between **Au12** and **Au10** was monitored by ^{1}H NMR spectroscopy and ESI-MS spectrometry in solution. Also reported here are DFT calculations on the mechanism of the unique interconversion between the ring-in-ring and [2]catenane structures; the results suggest that ligand-ligand dispersive interaction, as well as Au-Au orbital / Au-S orbital interactions, could be used to modulate supramolecular structures, in which the ligand-ligand and metal-ligand dispersive interactions synergically work with metal-metal/metal-ligand orbital interactions.

Results and Discussion

Treatment of Au(THT)Cl (THT = tetrahydrothiophene) with 9,9-dibutyl-fluorene-2-thiol (H$\boldsymbol{SC_4}$, 1 equiv) in CH_2Cl_2 in the presence of triethylamine gave a yellow solid. Extraction of the product with hexane, followed by removal of the solvent and recrystallization from CH_2Cl_2/MeCN afforded **Au10** in 83% yield as yellow needle crystals (Scheme 1). Interestingly, recrystallization of **Au10** from hexane, by slow evaporation of the hexane solution at room temperature for 7 days, afforded **Au12** in ~85% yield as yellow cubic crystals (Scheme 1); further recrystallization of **Au12** from CH_2Cl_2/MeCN converted it back to **Au10**. Such interconversion between **Au10** and **Au12** was not affected by oxygen, as the same interconversion was observed for both the systems under air and the systems under argon. The structures of **Au10** and **Au12** have been determined by single-crystal X-ray diffraction studies (Figure 2; Tables S1, S3, S4 in the Supporting Information).

Complex **Au10** has a [2]catenane structure (Figure 2a), the core of which (Figure 2b) contains two interlocked 10-membered Au_5S_5 metallamacrocycles with weak Au(I)···Au(I) interactions,

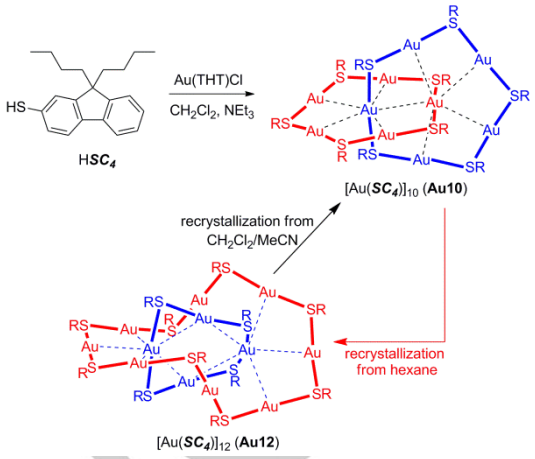

Scheme 1. Synthesis of **Au10** and **Au12** and their interconversion induced by solvents. Au···Au interactions are depicted as dashed lines.

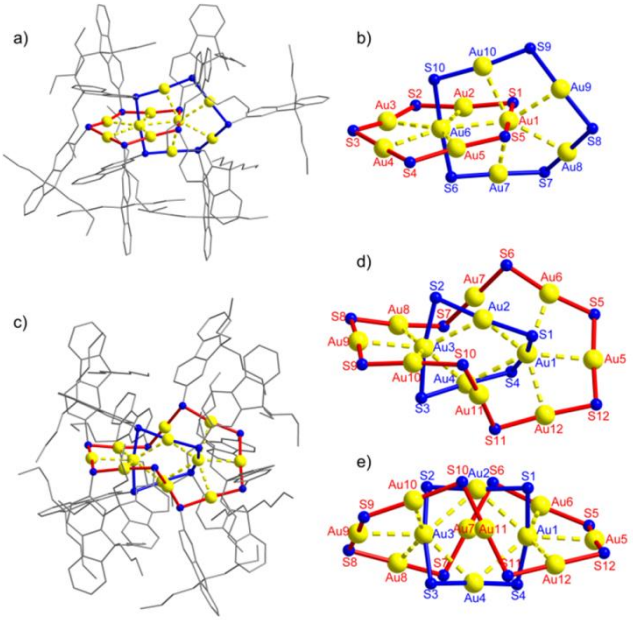

Figure 2. Crystal structures of **Au10** (a) along with its [2]catenane core (b), and **Au12** (c) together with its ring-in-ring core viewed along various directions (d, e). Au···Au interactions are depicted as dashed lines.

similar to the [2]catenane core of $[Au(SC_6H_4\text{-}\textit{p}\text{-}\textit{t}Bu)]_{10}$.[14] The nine close Au(I)···Au(I) contacts (< 3.3 Å, Table S3 in the Supporting Information) between the two Au_5S_5 metallamacrocycles of **Au10** average 3.038(6) Å, which is comparable to the average Au(I)···Au(I) contact of 3.05 Å in the crystal structure of $[Au(SC_6H_4\text{-}\textit{p}\text{-}\textit{t}Bu)]_{10}$.[14].

In contrast to **Au10**, complex **Au12** adopts a ring-in-ring structure, which consists of a $[Au(\boldsymbol{SC_4})]_4$ ring (Figure 3) and a $[Au(\boldsymbol{SC_4})]_8$ ring (Figure 4) apparently held together by weak Au(I)···Au(I) interactions (Figure 2c–e), with the $[Au(\boldsymbol{SC_4})]_4$ ring threading through the $[Au(\boldsymbol{SC_4})]_8$ ring. The ring-in-ring core of **Au12** viewed from different directions is depicted in Figure 2d,e.

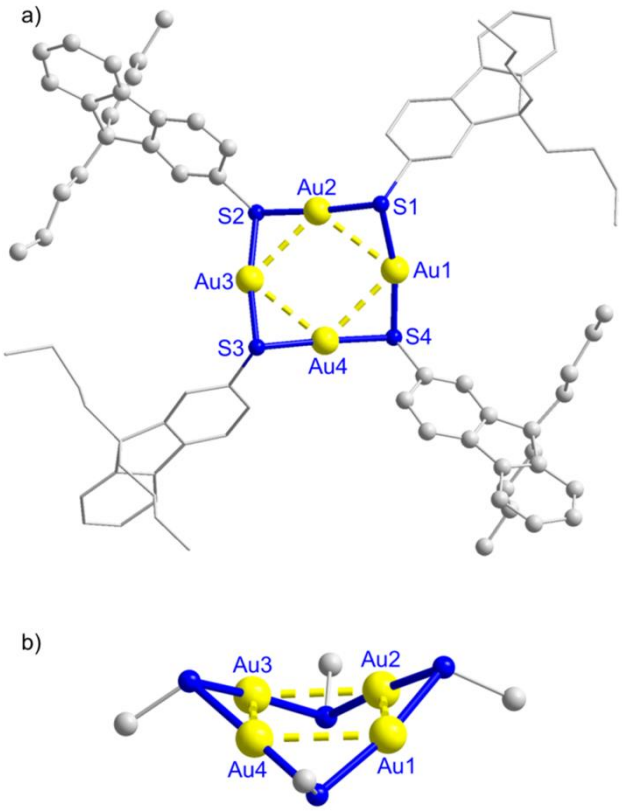

Figure 3. a) Structure of the inner [Au(***SC₄***)]$_4$ ring of **Au12**. Hydrogen atoms are not shown. The aryl groups (of the thiolate ligands) pointing backward are shown by stick representation. b) The 8-membered Au_4S_4 metallamacrocycle in the inner [Au(***SC₄***)]$_4$ ring viewed from a different direction depicting its butterfly-type conformation (all the thiolate aryl atoms, except the α carbons, are omitted).

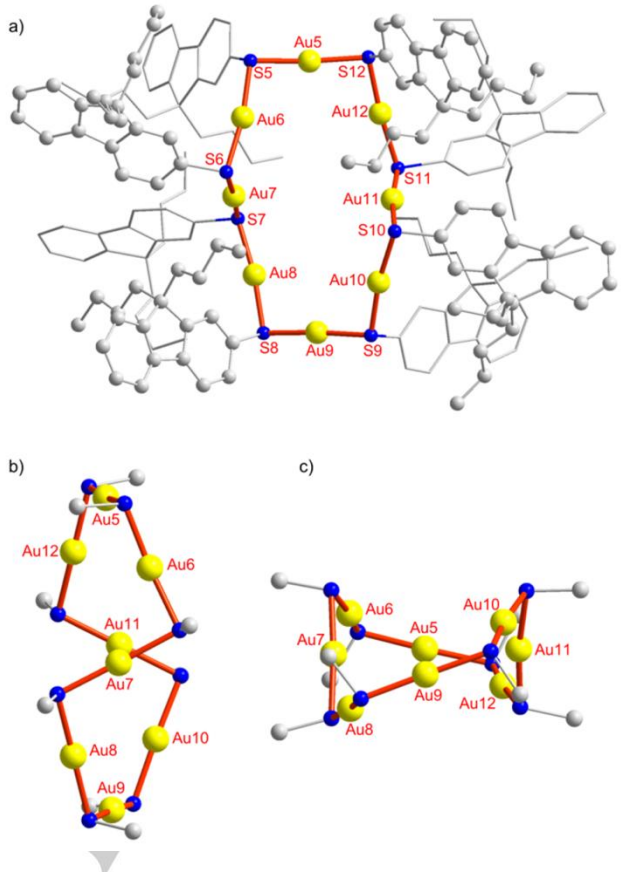

Figure 4. a) Structure of the outer [Au(***SC₄***)]$_8$ ring of **Au12**. Hydrogen atoms are not shown. The aryl groups (of the thiolate ligands) pointing backward are shown by stick representation. b) and c) The 16-membered Au_8S_8 metallamacrocycle in the outer [Au(***SC₄***)]$_8$ ring viewed from two different directions (all the thiolate aryl atoms, except the α carbons, are omitted).

The inner [Au(***SC₄***)]$_4$ ring of **Au12** features an 8-membered Au_4S_4 metallamacrocycle (Figure 3a) in a butterfly-type conformation (Figure 3b). The four gold atoms (Au1–Au4) are coplanar, and there are four close Au···Au contacts of 3.0412(7)–3.1433(7) Å (Table S4) within the [Au(***SC₄***)]$_4$ ring. Apart from these intra-ring Au(I)···Au(I) interactions, each of Au1 and Au3 shows three close Au···Au contacts with the Au atoms of the outer [Au(***SC₄***)]$_8$ ring of **Au12** (Figure 2d), and these six close Au···Au contacts between the inner and outer rings vary between 2.9225(7)–3.0675(7) Å. Probably owing to these six inter-ring Au···Au interactions, both the S1-Au1-S4 and S2-Au3-S3 moieties are appreciably bent (bond angles: 168.18(9)° and 169.24(9)°, respectively). The butterfly-type conformation of the 8-membered Au_4S_4 metallamacrocycle (with four intra-ring Au(I)···Au(I) interactions as mentioned above) observed for the [Au(***SC₄***)]$_4$ ring of **Au12** features a pair of substantially folded wings, with a fold angle (the angle between the two wing planes) of ~112°. In contrast, in the previously reported X-ray crystal structures of isolated cyclic [Au(SR)]$_4$ complexes,[19] the corresponding 8-membered Au_4S_4 metallamacrocycle adopts a slightly folded conformation in [AuS(Si{O*t*Bu}$_3$)]$_4$ (fold angle: ~157°)[19b] and a nearly planar conformation in [Au(SC{SiMe$_3$}$_3$)]$_4$[19a] and [Au(S{C_6H_4-*o*-X})]$_4$ (X = N=CHC_6H_4-*p*-NMe_2 or N=CH-mesityl).[19c]

The outer [Au(***SC₄***)]$_8$ ring of **Au12** features a unique, structurally characterized (by X-ray crystal analysis), 16-membered Au_8S_8 metallamacrocycle adopting a double-helical-like conformation (Figure 2e and Figure 4). Close Au···Au contacts (< 3.3 Å) are not observed within this 16-membered metallamacrocycle. In the literature, although there are several reports on computational studies involving *hypothetical* cyclic [Au(SR)]$_8$ species,[20] including a theoretically optimized double helical conformation for *hypothetical* [Au(SMe)]$_8$,[20b] *we could not find literature examples of cyclic [Au(SR)]$_8$ species that have been observed by experimental means.* The Au-S-Au angles in the [Au(***SC₄***)]$_8$ fall in the range of 91.98(11)–104.53(10)°; these angles are larger than the Au-S-Au angles in the [Au(***SC₄***)]$_4$ ring mentioned above. Compared with the *computed* double helical conformation for *hypothetical* [Au(SMe)]$_8$,[20b] which shows four pairs of Au atoms between the two helical components with the Au-Au separation within each pair being ~3.14–3.64 Å, the two helical-like components of the experimentally determined [Au(***SC₄***)]$_8$ ring of **Au12** are much less folded and feature three pairs of Au atoms (Au6-Au12, Au7-Au11, Au8-Au10, Figure 4b), with each pair showing a substantially larger Au-Au separation (~5.64, 6.16, and 5.86 Å, respectively).

The solution behavior of **Au10** and **Au12** was investigated by ESI-MS and ^{1}H NMR spectroscopy. The high-resolution ESI-MS spectrum shows a prominent cluster peak at *m*/*z* 5087.3628 for **Au10** (Figure S1) and at *m*/*z* 6099.5937 for **Au12** (Figure S2); these *m*/*z* values, together with the corresponding isotopic patterns, match those simulated for [**Au10** + Na]$^+$ and [**Au12** + Na]$^+$, respectively. The room-temperature ^{1}H NMR spectrum of **Au10** in CD_2Cl_2 or $CDCl_3$ displays three sets of aromatic resonances in a 2:4:4 ratio (Figure S4 and top of Figure 5, see also the ^{1}H-^{1}H COSY and NOESY NMR spectra depicted in Figures S7 and S8), which is consistent with the [2]catenane structure of **Au10** wherein the 10 thiolate ligands are divided into three groups in a 2:4:4 ratio based on their environments, reminiscent of the case of Au(I)-alkynyl [2]catenanes $[Au(C{\equiv}CR)]_{10}$.[13] The ^{1}H NMR spectrum of **Au12** in CD_2Cl_2 (Figure S5) or $CDCl_3$ (bottom of Figure 5) is more complex than that of **Au10**, a comparison of their signals is depicted in Figure S6. We also measured the variable-temperature ^{1}H NMR spectra of **Au12** in $CDCl_3$ (Figure S14), which revealed that the signals of **Au12** disappeared upon increasing temperature to 328 K with the signals observed at this temperature, and also at 338 K, being identical to those of **Au10**. Upon lowering temperature from 338 K to room temperature, the signals remained identical to those of **Au10**; no signals of **Au12** were recovered. These measurements suggest conversion of **Au12** to **Au10** in $CDCl_3$, a cluster-to-cluster transformation in solution, upon increase of temperature (Scheme 2).

To better understand the cluster-to-cluster transformation process, we monitored a solution of **Au12** in $CDCl_3$ at room temperature by measuring its ^{1}H NMR spectra (1,2-dichloroethane as internal standard) at different times (Figure 5). As shown in Figure 5, the signals at δ 8.46, 8.27 and 6.85 ppm of **Au12** gradually disappeared, while those at δ 7.83 and 6.94 ppm of **Au10** gradually grew, with increasing time, indicating a

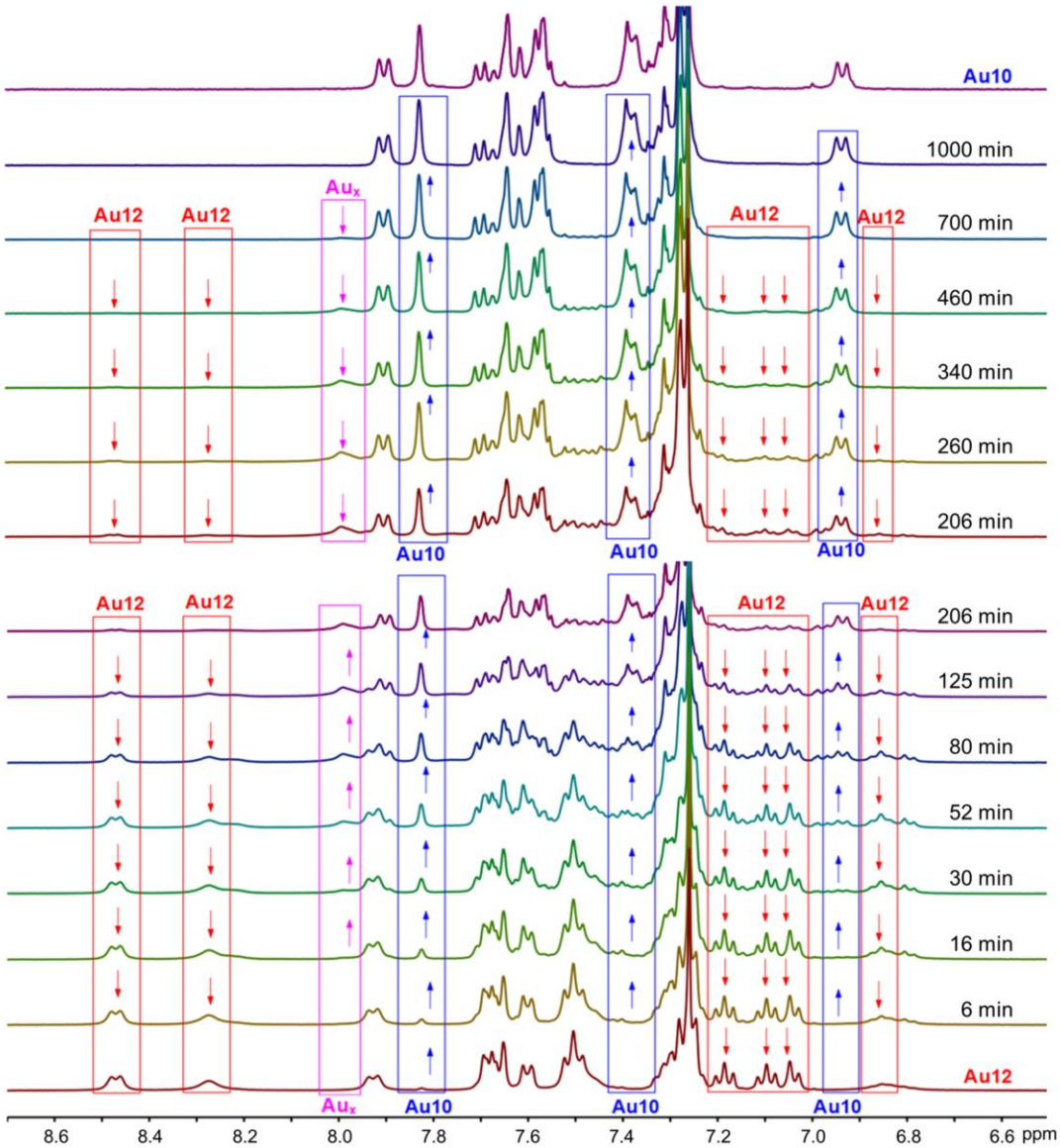

Figure 5. ^{1}H NMR (400 MHz) spectra (in aromatic region), in $CDCl_3$ at 298 K, of **Au10** (top), **Au12** (bottom; 2.1 × 10^{-3} M; 1,2-dichloroethane as internal standard), and the solution of **Au12** upon standing for different times (spectra between top and bottom).

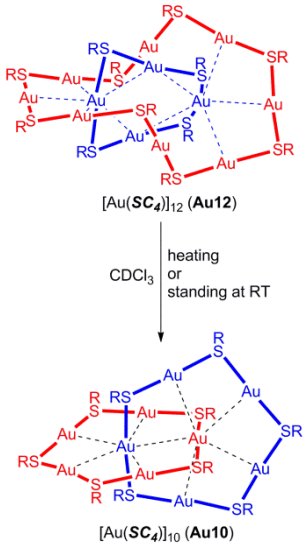

Scheme 2. Ring-in-ring cluster **Au12** to [2]catenane cluster **Au10** transformation in $CDCl_3$. Au(I)···Au(I) interactions are depicted as dashed lines.

gradual transformation of **Au12** to **Au10** in the solution at room temperature (Scheme 2), and the transformation was completed within 1000 min under these conditions. Based on the integration ratios relative to the internal standard, the conversion of **Au12** to **Au10** is virtually quantitative. The variable-time spectral changes in Figure 5 also revealed generation of intermediate species during the cluster core transformation in solution. In the spectrum measured at 16 min, a signal at 7.99 ppm belonging to neither **Au10** nor **Au12** appeared; this signal, which reached its maximum after ~206 min and then started to vanish gradually, belongs to a new species $\mathbf{Au_x}$, presumably a $[Au(\boldsymbol{SC_4})]_n$ ($n \neq 10$ and 12) cluster. After 1000 min, all the peaks attributed to **Au12** and $\mathbf{Au_x}$ disappeared, and only the signals corresponding to **Au10** were observed. We further examined the room-temperature ^{1}H DOSY NMR spectra of two mixtures of **Au12**, $\mathbf{Au_x}$, and **Au10** in $CDCl_3$ which were obtained from a solution of **Au12** in $CDCl_3$ after standing for ~30 and ~120 min (Figures S11–S13); these DOSY NMR measurements revealed that the molecules of **Au10**, **Au12** and $\mathbf{Au_x}$ have comparable diffusion constants (~4 × 10^{-10} m^2/s), indicating that the molecular size of $\mathbf{Au_x}$ is comparable to that of **Au10** and **Au12**. The intermediate species $\mathbf{Au_x}$ was only observed in solution; our attempts to isolate this species in pure form have not been successful.

We then monitored the cluster core transformation process (**Au12** → **Au10**) by ESI-MS measurements (Figure 6). The freshly prepared **Au12** solution in CH_2Cl_2/MeOH features one prominent cluster peak attributed to [**Au12** + Na]$^+$, along with two weak cluster peaks attributable to [**Au10** + Na]$^+$ and {$[Au(\boldsymbol{SC_4})]_{11}$ (**Au11**) + Na}$^+$ (Figure 6a). After 65 min, the peaks attributable to [**Au10** + Na]$^+$ and [**Au11** + Na]$^+$ increased, and at 90 min, the ESI-MS spectrum features two prominent peaks assigned to [**Au10** + Na]$^+$ and [**Au12** + Na]$^+$, indicating a considerable transformation of **Au12** to **Au10**. Then, at ~150 min, the peak of [**Au12** + Na]$^+$ decreased, while the peak of [**Au11** + Na]$^+$ reached its maximum and began to decrease. Finally, after 400

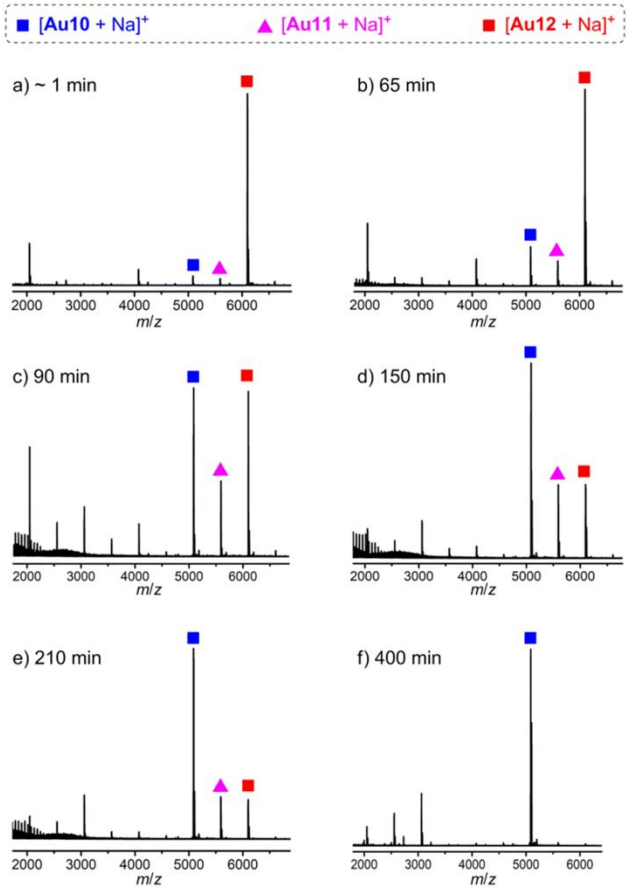

Figure 6. ESI-MS spectral changes of **Au12** in CH_2Cl_2/MeOH.

min, the spectrum features the prominent peak of [**Au10** + Na]$^+$, and the two peaks of [**Au11** + Na]$^+$ and [**Au12** + Na]$^+$ disappeared. On the basis of these ESI-MS measurements and the NMR studies described above, the new complex $\mathbf{Au_x}$ appeared in the ^{1}H NMR spectra (Figure 5), which appeared as an intermediate in the **Au12**-to-**Au10** transformation process, is likely to be $[Au(\boldsymbol{SC_4})]_{11}$ (**Au11**).

Given the different numbers of Au atoms in **Au10** and **Au12**, the transformations between the two clusters do not belong to isomerization processes. We noted that, in both the cluster cores of **Au10** and **Au12**, there are 10 Au atoms connected by a total of 10 close Au···Au contacts (< 3.3 Å), and **Au12** has two extra Au atoms which are not involved in the 10 close contacts. Thus, as one of the possible pathways for the transformation of **Au12** to **Au10**, cluster **Au10** might come from a rearrangement of the '$[Au(\boldsymbol{SC4})]_{10}$' moiety of **Au12** connected by the close Au···Au contacts. If such is the case, the two extra '$[Au(\boldsymbol{SC_4})]$' moieties dissociated from **Au12**, possibly via intermediate **Au11**, would self-assemble to also give **Au10** in $CDCl_3$ under the conditions employed, as **Au12** was quantitatively converted to **Au10** upon standing in $CDCl_3$. On the other hand, the transformation of **Au10** to **Au12** upon slow crystallization from hexane suggests that the **Au10** cluster is likely to undergo some extent of dissociation in the solution to generate, for example, transient mononuclear '$[Au(\boldsymbol{SC_4})]$' species that can add to a **Au10** molecule to form **Au11** and/or **Au12** (the '$[Au(\boldsymbol{SC_4})]$'

species was not directly detected by spectroscopic means such as NMR measurements, possibly owing to insufficiently long lifetime and/or too low concentration).

The transformation from **Au10** to **Au12** in solution was also inspected by recrystallization of **Au10** from various other solvents, including pentane, petroleum ether (40–60 °C), diethyl ether, methyl *tert*-butyl ether, and benzene for several days, with the products (after removal of the solvents) redissolved in $CDCl_3$ immediately being examined by ^{1}H NMR spectroscopy. From the NMR spectra obtained (Figure S15), **Au12** could also be formed by slow recrystallization of **Au10** from pentane and the petroleum ether, but not from diethyl ether, methyl *tert*-butyl ether, and benzene. It was found that, in the solvents CH_2Cl_2, $CHCl_3$, CH_2Cl_2/MeCN, diethyl ether, methyl *tert*-butyl ether, and benzene, which either bear highly electronegative Cl, N, or O atom(s) capable of forming hydrogen bonds or feature aromatic ring capable of participating in π-π interactions, both **Au10** and **Au12** are well soluble with the former being more stable (as reflected by the gradual transformation of **Au12** to **Au10** in these solutions). However, in hexane, pentane, and petroleum ether (40–60 °C), which bear neither aromatic groups nor highly electronegative atoms, only **Au10** has a good solubility whereas **Au12** is virtually insoluble; thus, the transformation of **Au10** in these alkane solvents to **Au12** was probably driven by the precipitation of **Au12** from the solution system.

The effect of thiolate ligands on the self-assembly of **Au10** and **Au12** was examined by using several congeners of H***SC₄***, including H***SC*** $_m$ (***m*** = **1**, **2**, **3**, **6**; Scheme 3). Reactions of Au(THT)Cl with these thiols under the conditions identical to those for H***SC₄*** gave [Au(***SC*** $_m$)]$_{10}$ (**m** = **1**, **2**, **3**, **6**) which are the [2]catenane congeners of **Au10** as revealed by ESI-MS and ^{1}H NMR spectroscopy. For example, the HR ESI-MS spectra of [Au(***SC*** $_m$)]$_{10}$ (***m*** = **1**, **2**, **3**) feature a prominent cluster peak attributable to {[Au(***SC₁***)]$_{10}$ + Na}$^+$ (Figure S16), {[Au(***SC₂***)]$_{10}$ + Na}$^+$ (Figure S18) and {[Au(***SC₃***)]$_{10}$ + H}$^+$ (Figure S20), respectively. The ^{1}H NMR spectrum of [Au(***SC₁***)]$_{10}$ in $CDCl_3$ (Figure S17) shows three sets of its thiolate ligand signals in a 2:4:4 ratio, reminiscent of that of **Au10**. Recrystallization of [Au(***SC*** $_m$)]$_{10}$ (***m*** = **1**, **2**, **3**) from different solvents, including hexane, petroleum ether, CH_2Cl_2/MeOH, and CH_2Cl_2/CH_3CN only afforded powders which showed the same ESI-MS and ^{1}H NMR spectra of the starting [2]catenanes, without producing the corresponding ring-in-ring clusters (Scheme 3). In the case of [Au(***SC₆***)]$_{10}$, recrystallization from CH_2Cl_2/MeCN afforded needle crystals; its X-ray crystal structure was determined (Figure S24), revealing that this cluster adopts a [2]catenane structure. Upon slow recrystallization from hexane for ~7 days, the resulting powder showed an ESI-MS spectrum featuring two prominent cluster peaks attributable to {[Au(***SC₆***)]$_{10}$ + Na}$^+$ and {[Au(***SC₆***)]$_{12}$ + Na}$^+$ (Figure S25), and gave a ^{1}H NMR spectrum (in $CDCl_3$ at room temperature, Figure S26) analogous to that of a mixture of **Au10** and **Au12**, suggesting the possible formation of a ring-in-ring [Au(***SC₆***)]$_{12}$ cluster by recrystallization of [Au(***SC₆***)]$_{10}$ from hexane. Also, variable-temperature ^{1}H NMR measurements (Figure S27) revealed facile transformation of the proposed ring-in-ring [Au(***SC₆***)]$_{12}$ to [2]catenane [Au(***SC₆***)]$_{10}$ in $CDCl_3$ upon increasing temperature to 340 K, and by cooling back to room temperature, the signals remained identical to those of [Au(***SC₆***)]$_{10}$.

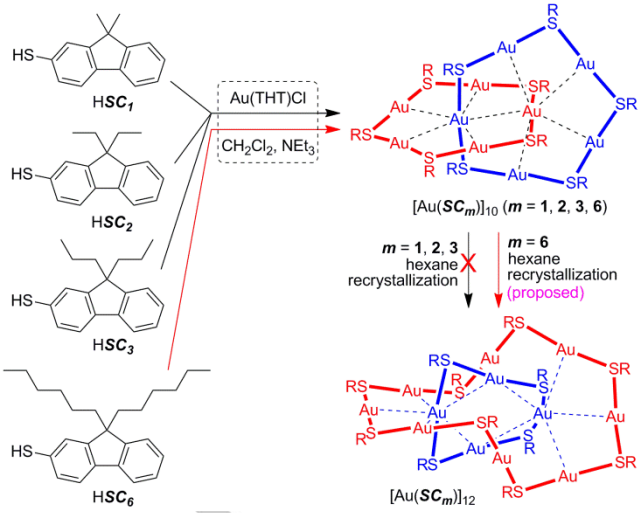

Scheme 3. Effect of thiolate ligands.

DFT calculations together with the energy decomposition analysis (EDA)[21,22] were performed to gain insight into the transformation between [2]catenane [Au(SR)]$_{10}$ and ring-in-ring [Au(SR)]$_{12}$ (SR = ***SC₄***; **Au10** and **Au12**, respectively). From the computational studies and based on the experimental evidence (e.g. Figures 5 and 6 and structure features of **Au10** and **Au12**), a stepwise pathway for the interconversion between **Au10** and **Au12** is proposed (Figure 7a, steps I–V), though the possible involvement of a more concerted pathway featuring recombination/dissociation of oligomeric units could not be excluded. The computed energies for each step are depicted in Figure 7b and the stabilization energy per monomer of the reaction intermediates is shown in Figure 7c. As shown in Figure 7a, for the expansion of the [Au(SR)]$_{10}$ cluster **Au10** in hexane, we considered that an exterior [Au(SR)] unit (Au is highlighted in red), which can possibly be generated by some extent of dissociation of **Au10** in solution as mentioned above, is inserted into the seam between the two interlocked rings ("5+5" gold thiolate [2]catenane), resulting in the "5+5+1" core structure of [Au(SR)]$_{11a}$ (stability discussed below), the space-filling diagram of which is depicted in Figure S29. The added Au of [Au(SR)] can form direct interactions with the nearby Au and S with a distance of 3.20 Å (Au···Au) and 2.33 Å (Au···S). The expansion of the cluster is energetically favorable with an energy decrease of 1.88 eV due to introducing additional Au···Au and Au···S interactions. The stable [Au(SR)]$_{11a}$ was proposed to account for the signal of the **Au11** species in the mass spectra (Figure 6). Inevitably, the insertion of a new [Au(SR)] monomer makes the cluster more crowded. As a consequence, a second exterior [Au(SR)] binding to the [Au(SR)]$_{11a}$, i.e., the formation of the "5+5+1+1" skeleton is hindered due to steric limitations in the following step. This means that a structure distortion based on the "5+5+1" core is needed for the further expansion of the cluster. Inspired by our previous studies on the [2]catenane [Au(SR)]$_{11}$ consisting of interlocked [Au_5S_5] and [Au_6S_6] rings,[15] a [2]catenane species [Au(SR)]$_{11b}$ ("5+6") is proposed to be generated. Based on the DFT calculated energy, the [Au(SR)]$_{11a}$ → [Au(SR)]$_{11b}$ transformation process is endothermic. The EDA

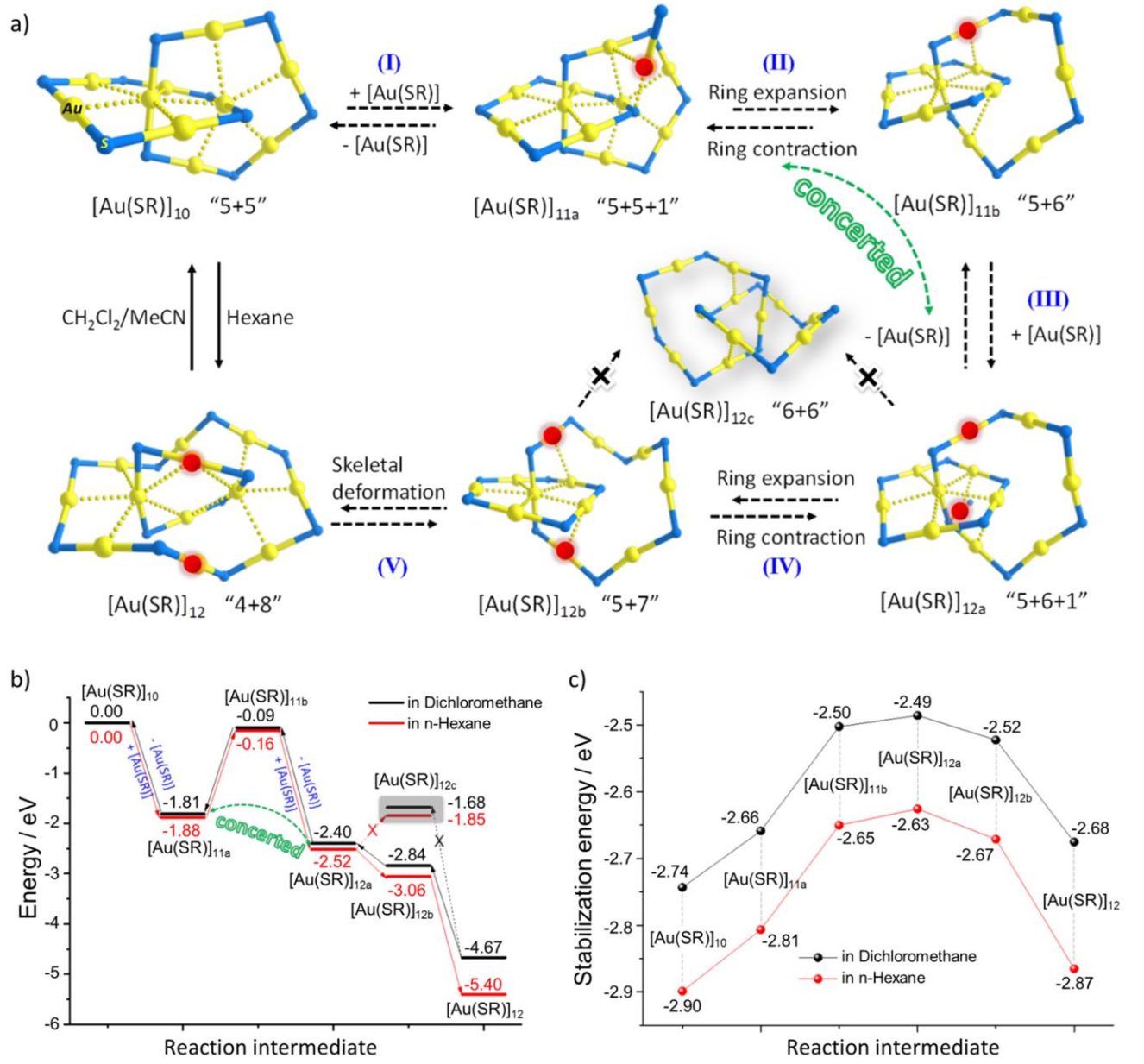

Figure 7. a) Proposed intermediate structures for the step-by-step transformation between $[Au(SR)]_{10}$ and $[Au(SR)]_{12}$ (SR = ***SC$_4$***). Only the Au-S skeletons are shown for clarity (full structures are depicted in Figure S30). The exterior Au of [Au(SR)] is illustrated by a red ball. (Color labels: yellow = Au and blue = S). b) Computed energies for each conversion step described in a). c) Stabilization energy per monomer of the reaction intermediates.

analysis of $[Au(SR)]_{11a}$ and $[Au(SR)]_{11b}$ species revealed that the weakened orbital interaction and dispersion interaction are the origin of the increase in energy (Table S6). The EDA results also confer a smaller steric repulsion effect of $[Au(SR)]_{11b}$ (19.78 eV) than that of $[Au(SR)]_{11a}$ (21.72 eV). The decreased repulsion also provides a possibility for a further expansion of $[Au(SR)]_{11b}$.

Following the cluster core rearrangement of $[Au(SR)]_{11a}$ in step II, the second [Au(SR)] unit is introduced to form $[Au(SR)]_{12a}$ ("5+6+1"; for its space-filling diagram, see Figure S29) with the intense thermal release of 2.36 eV. Considering the large energy barrier in $[Au(SR)]_{11a} \rightarrow [Au(SR)]_{11b}$ ring expansion (step II), the transformation of $[Au(SR)]_{11a}$ to $[Au(SR)]_{12a}$ could possibly proceed in a concerted energy-saving manner (Figure 7a,b). Subsequent ring expansion can lead to [2]catenane $[Au(SR)]_{12b}$ ("5+7") or $[Au(SR)]_{12c}$ ("6+6"). The DFT results revealed that the transformation to $[Au(SR)]_{12b}$ ("5+7") is energetically favorable whereas the transformation to $[Au(SR)]_{12c}$ ("6+6") is unfavorable (see Figure 7b). Finally, $[Au(SR)]_{12}$ ("4+8", **Au12**) can be generated through a further skeletal transformation from $[Au(SR)]_{12b}$ ("5+7"). The rearrangements along the $[Au(SR)]_{12a} \rightarrow [Au(SR)]_{12b} \rightarrow [Au(SR)]_{12}$ evolution direction is along an energy downhill pathway. The EDA results

show that although the $[Au(SR)]_{12a} \rightarrow [Au(SR)]_{12b} \rightarrow [Au(SR)]_{12}$ conversion shows increased steric repulsion, this energy is entirely compensated by the strengthened orbital interactions and dispersion effects of the ***SC4*** ligands (see Figure S32 and Table S7). However, the improved steric repulsion for the [2]catenane $[Au(SR)]_{12c}$ cannot be well compensated due to the limited binding interactions, making it less prevalent species. The energy changes in each step for the transformation from $[Au(SR)]_{10}$ (**Au10**) to $[Au(SR)]_{12}$ (**Au12**) is shown in Figure 7b. Accordingly, the reverse process indicates that the $[Au(SR)]_{12}$ can transform to the $[Au(SR)]_{10}$ cluster via ring contraction reaction and two [Au(SR)] units elimination. From $[Au(SR)]_{12}$ to $[Au(SR)]_{10}$, the elimination of the [Au(SR)] unit was found to be the rate-determining step.

To gain further insight into the driven force of the cluster expansion of **Au10**, the stabilization energy E_{stabl} was calculated based on the DFT energies. The stabilization energy calculations for the reaction intermediates reveal that $[Au(SR)]_{10}$ (**Au10**) is the most stable species, which affords the largest stabilization energy per monomer in solution (Figure 7c). It can also be noted that the stabilization energy of $[Au(SR)]_{11a}$ (**Au11**) and $[Au(SR)]_{12}$ (**Au12**) is slightly higher (< 0.10 eV) than that of $[Au(SR)]_{10}$, implying that these two species are also possible to be experimentally observed. The small stabilization energy differences (0.06 eV in dichloromethane and 0.03 eV in hexane) between $[Au(SR)]_{10}$ and $[Au(SR)]_{12}$ also afford the possibility for the solvent-induced transformations between the two clusters.

Brisdon and co-workers previously reported Au(I)-thiolate [2]catenane $[Au(SC_6H_4\text{-}o\text{-}CMe_3)]_{12}$.[14] Our attempts to obtain its ***SC4*** counterpart, i.e., the [2]catenane $[Au(SR)]_{12c}$ (SR = ***SC4***), have been unsuccessful. To computationally gain insight behind the phenomenon, we built up four models based on the X-ray crystal structures of **Au12** (in this work) and $[Au(SC_6H_4\text{-}o\text{-}CMe_3)]_{12}$ (reported by Brisdon and co-workers[14]): the ***SC4***-capped "8+4" ring-in-ring cluster **1** and hypothetical "6+6" [2]catenane cluster **2**; the SC_6H_4-*o*-CMe_3-coordinated "6+6" [2]catenane cluster **3** and hypothetical "8+4" ring-in-ring cluster **4** (Figure 8). The energy calculations on these four clusters show that cluster **1** is more stable than cluster **2**. The EDA analysis revealed that, although cluster **1** has a larger steric repulsion, this is offset by a greater dispersion effect of the ***SC4*** ligands (Table S8). In contrast, the rather large steric repulsion for cluster **4** cannot be well compensated by its ligand-induced orbital and dispersion interactions; therefore, cluster **3** is more stable than cluster **4**. These calculation results provide a possible rationalization for the ring-in-ring structure of $[Au(\textbf{\textit{SC4}})]_{12}$ observed in this work but a [2]catenane structure of $[Au(SC_6H_4\text{-}o\text{-}CMe_3)]_{12}$ reported previously.[14] Thus, variation of thiolate ligands can afford dramatic changes on the stability of the Au(I)-thiolate clusters by changing the strength of the individual energy of interaction components, indicating ligand-dependent stability for the Au(I)-thiolate cluster cores.

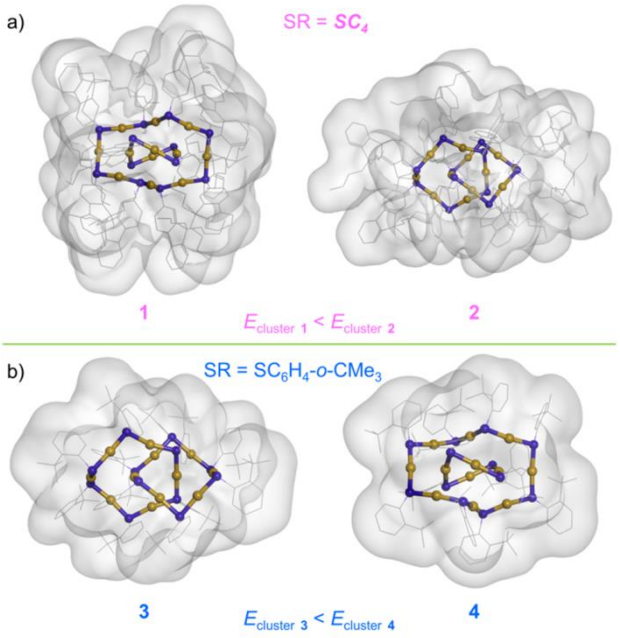

Figure 8. Energy comparison between ring-in-ring ("8+4") and [2]catenane ("6+6") structures of DFT-computed $[Au(SR)]_{12}$ clusters for a) SR = ***SC4*** (**1** and **2**) and b) SR = SC_6H_4-*o*-CMe_3 (**3** and **4**). The Au···Au interactions are not shown. The geometry of the ring-in-ring cluster core (Au-S skeleton) for **1** and **4** was taken from the crystal structure of **Au12** in this work, whereas that of the [2]catenane core (Au-S skeleton) for **2** and **3** was taken from the crystal structure of $[Au(SC_6H_4\text{-}o\text{-}CMe_3)]_{12}$,[14] without optimization; the geometry of the R groups in **1**–**4** was optimized.

Conclusion

A gold(I)-thiolate ring-in-ring cluster $[Au(\textbf{\textit{SC4}})]_{12}$ (**Au12**), stabilized by weak Au(I)···Au(I) interactions and a bulky dibutyl-fluorene-2-thiolate ligand (***SC4***), has been obtained by cluster core transformation of the [2]catenane $[Au(\textbf{\textit{SC4}})]_{10}$ (**Au10**) in alkane solvents such as hexane. Dissolution of **Au12** in CH_2Cl_2 or $CHCl_3$ reversed the cluster core transformation process, converting **Au12** back to **Au10**. By monitoring the transformation between **Au12** and **Au10** in solution by ^{1}H NMR and ESI-MS analysis, a $[Au(\textbf{\textit{SC4}})]_{11}$ (**Au11**) species is suggested to be a possible intermediate in the **Au12**-to-**Au10** transformation. DFT calculations revealed that the expansion of **Au10** to **Au12** is likely to proceed in a stepwise manner via generation of $[Au(\textbf{\textit{SC4}})]_{11}$ (**Au11**) intermediate species, and change of the thiolate ligands can alter the strength of steric, orbital, and dispersive interactions resulting in dramatic changes on the structure types of Au(I)-thiolate cluster cores. Complex **Au12** consists of an 8-membered $[Au(\textbf{\textit{SC4}})]_4$ metallamacrocycle and a 16-membered $[Au(\textbf{\textit{SC4}})]_8$ metallamacrocycle; the former adopts a markedly different conformation from those of literature reported cyclic $[Au(SR)]_4$ clusters whereas for the latter, no experimentally observed cyclic $[Au(SR)]_8$ clusters have been reported previously. The present work not only provides a structure type unprecedented for Au(I)-thiolate clusters (i.e. ring-in-ring structure such as **Au12**), but also contributes a unique type of ring-in-ring metal complexes, in which the noninterlocked rings are linked by weak metallophilic interactions.

Acknowledgements

This work was supported by Hong Kong Research Grants Council (HKU 17300518) and Basic Research Program-Shenzhen Fund (JCYJ20160229123546997, JCYJ20170412140251576, JCYJ20170818141858021, and JCYJ20180508162429786).

Conflict of interest

The authors declare no conflict of interest.

Keywords: gold(I) • metallophilic interactions • ring-in-ring complexes • supramolecular assemblies • thiolates

[1] a) D. B. Amabilino, J. F. Stoddart, *Chem. Rev*. **1995**, *95*, 2725-2828; b) V. Balzani, A. Credi, F. M. Raymo, J. F. Stoddart, *Angew. Chem. Int. Ed*. **2000**, *39*, 3348-3391; *Angew. Chem.* **2000**, *112*, 3484-3530; c) V. Balzani, A. Credi, S. Silvi, M. Venturi, *Chem. Soc. Rev*. **2006**, *35*, 1135-1149; d) S. Erbas-Cakmak, D. A. Leigh, C. T. McTernan, A. L. Nussbaumer, *Chem. Rev*. **2015**, *115*, 10081-10206; e) A. J. McConnell, C. S. Wood, P. P. Neelakandan, J. R. Nitschke, *Chem. Rev*. **2015**, *115*, 7729-7793; f) E. R. Kay, D. A. Leigh, *Angew. Chem. Int. Ed*. **2015**, *54*, 10080-10088; *Angew. Chem.* **2015**, *127*, 10218-10226; g) W. Wang, Y.-X. Wang, H.-B. Yang, *Chem. Soc. Rev*. **2016**, *45*, 2656-2693.

[2] a) M. Fujita, *Acc. Chem. Res.* **1999**, *32*, 53-61; b) G. Gil-Ramírez, D. A. Leigh, A. J. Stephens, *Angew. Chem. Int. Ed.* **2015**, *54*, 6110-6150; *Angew. Chem.* **2015**, *127*, 6208-6249; c) J. E. M. Lewis, P. D. Beer, S. J. Loeb, S. M. Goldup, *Chem. Soc. Rev*. **2017**, *46*, 2577-2591.

[3] a) S.-H. Chiu, A. R. Pease, J. F. Stoddart, A. J. P. White, D. J. Williams, *Angew. Chem*. *Int. Ed.* **2002**, *41*, 270-274; *Angew. Chem*. **2002**, *114*, 280-284; b) S. J. Cantrill, K. S. Chichak, A. J. Peters, J. F. Stoddart, *Acc. Chem. Res*. **2005**, *38*, 1-9; c) R. S. Forgan, C. Wang, D. C. Friedman, J. M. Spruell, C. L. Stern, A. A. Sarjeant, D. Cao, J. F. Stoddart, *Chem. Eur. J.* **2012**, *18*, 202-212; d) J. Sun, M. Frasconi, Z. Liu, J. C. Barnes, Y. Wang, D. Chen, C. L. Stern, J. F. Stoddart, *Chem. Commun.* **2015**, *51*, 1432-1435.

[4] a) S. Kamitori, K. Hirotsu, T. Higuchi, *J. Am. Chem. Soc.* **1987**, *109*, 2409-2414; b) S.-Y. Kim, I.-S. Jung, E. Lee, J. Kim, S. Sakamoto, K. Yamaguchi, K. Kim, *Angew. Chem. Int. Ed.* **2001**, *40*, 2119-2121; *Angew. Chem.* **2001**, *113*, 2177-2179; c) A. I. Day, R. J. Blanch, A. P. Arnold, S. Lorenzo, G. R. Lewis, I. Dance, *Angew. Chem. Int. Ed.* **2002**, *41*, 275-277; *Angew. Chem.* **2002**, *114*, 285-287; d) T. Kawase, K. Tanaka, N. Shiono, Y. Seirai, M. Oda, *Angew. Chem. Int. Ed.* **2004**, *43*, 1722-1724; *Angew. Chem.* **2004**, *116*, 1754-1756; e) S. J. Dalgarno, J. Fisher, C. L. Raston, *Chem. Eur. J.* **2006**, *12*, 2772-2777; f) T. Kawase, Y. Nishiyama, T. Nakamura, T. Ebi, K. Matsumoto, H. Kurata, M. Oda, *Angew. Chem. Int. Ed.* **2007**, *46*, 1086-1088; *Angew. Chem.* **2007**, *119*, 1104-1106; g) S. A. L. Rousseaux, J. Q. Gong, R. Haver, B. Odell, T. D. W. Claridge, L. M. Herz, H. L. Anderson, *J. Am. Chem. Soc.* **2015**, *137*, 12713-12718; h) K. Cai, M. C. Lipke, Z. Liu, J. Nelson, T. Cheng, Y. Shi, C. Cheng, D. Shen, J.-M. Han, S. Vemuri, Y. Feng, C. L. Stern, W. A. Goddard III, M. R. Wasielewski, J. F. Stoddart, *Nat. Commun.* **2018**, *9*, 5275/1-5275/8.

[5] M. C. Lipke, Y. Wu, I. Roy, Y. Wang, M. R. Wasielewski, J. F. Stoddart, *ACS Central Sci.* **2018**, *4*, 362-371.

[6] For examples of ring-in-ring structures in which the rings are held together by covalent bonds, see: a) J.-H. Fu, Y.-H. Lee, Y.-J. He, Y.-T. Chan, *Angew. Chem. Int. Ed.* **2015**, *54*, 6231-6235; *Angew. Chem.* **2015**, *127*, 6329-6333; b) B. Sun, M. Wang, Z. Lou, M. Huang, C. Xu, X. Li, L.-J. Chen, Y. Yu, G. L. Davis, B. Xu, H.-B. Yang, X. Li, *J. Am. Chem. Soc.* **2015**, *137*, 1556-1564; c) M. Wang, K. Wang, C. Wang, M. Huang, X.-Q. Hao, M.-Z. Shen, G.-Q. Shi, Z. Zhang, B. Song, A. Cisneros, M.-P. Song, B. Xu, X. Li, *J. Am. Chem. Soc.* **2016**, *138*, 9258-9268; d) H. Wang, X. Qian, K. Wang, M. Su, W.-W. Haoyang, X. Jiang, R. Brzozowski, M. Wang, X. Gao, Y. Li, B. Xu, P. Eswara, X.-Q. Hao, W. Gong, J.-L. Hou, J. Cai, X. Li, *Nat. Commun.* **2018**, *9*, 1815/1-1815/9; e) S. Chakraborty, G. R. Newkome, *Chem. Soc. Rev.* **2018**, *47*, 3991-4016; f) C. Wei, Y. He, X. Shi, Z. Song, *Coord. Chem. Rev.* **2019**, *385*, 1-19.

[7] a) T. J. Hubin, A. G. Kolchinski, A. L. Vance, D. H. Busch, *Adv. Supramol. Chem*. **1999**, *5*, 237; b) J. C. Loren, M. Yoshizawa, R. F. Haldimann, A. Linden, J. S. Siegel, *Angew. Chem. Int. Ed*. **2003**, *42*, 5702-5705; *Angew. Chem.* **2003**, *115*, 5880-5883; c) R. S. Forgan, J. M. Spruell, J.-C. Olsen, C. L. Stern, J. F. Stoddart, *J. Mex. Chem. Soc*. **2009**, *53*, 134-138; d) J. Veliks, H. M. Seifert, D. K. Frantz, J. K. Klosterman, J.-C. Tseng, A. Linden, J. S. Siegel, *Org. Chem. Front*. **2016**, *3*, 667-672; e) S.-L. Huang, T. S. A. Hor, G.-X. Jin, *Coord. Chem. Rev*. **2017**, *333*, 1-26.

[8] a) M. Schmittel, A. Ganz, D. Fenske, *Org. Lett*. **2002**, *4*, 2289-2292; b) J. K. Klosterman, J. Veliks, D. K. Frantz, Y. Yasui, M. Loepfe, E. Zysman-Colman, A. Linden, J. S. Siegel, *Org. Chem. Front.* **2016**, *3*, 661-666.

[9] a) R. S. Forgan, D. C. Friedman, C. L. Stern, C. J. Bruns, J. F. Stoddart, *Chem. Commun*. **2010**, *46*, 5861-5863; b) V. Vajpayee, Y. H. Song, T. R. Cook, H. Kim, Y. Lee, P. J. Stang, K.-W. Chi, *J. Am. Chem. Soc*. **2011**, *133*, 19646-19649; c) M. Frasconi, T. Kikuci, D. Cao, Y. Wu, W.-G. Liu, S. M. Dyar, G. Barin, A. A. Sarjeant, C. L. Stern, R. Garmieli, C. Wang, M. R. Wasielewski, W. A. Goddard, III, J. F. Stoddart, *J. Am. Chem. Soc*. **2014**, *136*, 11011-11026; d) N. Singh, D. Kim, D. H. Kim, E.-H. Kim, H. Kim, M. S. Lah, K.-W. Chi, *Dalton Trans*. **2017**, *46*, 571-577.

[10] a) Y. Liu, *Tetrahedron Lett*. **2007**, *48*, 3871-3874; b) C. Alvariño, C. Platas-Iglesias, V. Blanco, M. D. García, C. Peinador, J. M. Quintela, *Dalton Trans.* **2016**, *45*, 11611-11615.

[11] P. Pyykkö, *Chem. Rev*. **1997**, *97*, 597-636.

[12] D. M. P. Mingos, J. Yau, S. Menzer, D. J. Williams, *Angew. Chem. Int. Ed.* **1995**, *34*, 1894-1895; *Angew. Chem.* **1995**, *107*, 2045-2047.

[13] I. O. Koshevoy, Y.-C. Chang, A. J. Karttunen, S. I. Selivanov, J. Jänis, M. Haukka, T. Pakkanen, S. P. Tunik, P.-T. Chou, *Inorg. Chem*. **2012**, *51*, 7392-7403.

[14] M. R. Wiseman, P. A. Marsh, P. T. Bishop, B. J. Brisdon, M. F. Mahon, *J. Am. Chem. Soc.* **2000**, *122*, 12598-12599.

[15] S. S.-Y. Chui, R. Chen, C.-M. Che, *Angew. Chem. Int. Ed.* **2006**, *45*, 1621-1624; *Angew. Chem.* **2006**, *118* 1651-1654.

[16] a) C. P. McArdle, S. Van. M. C. Jennings, R. J. Puddephatt, *J. Am. Chem. Soc*. **2002**, *124*, 3959-3965; b) R. J. Puddephatt, *J. Organomet. Chem.* **2015**, *792*, 13-24.

[17] X.-Y. Chang, G.-T. Xu, B. Cao, J.-Y. Wang, J.-S. Huang, C.-M. Che, *Chem. Sci.* **2017**, *8*, 7815-7820.

[18] S. S.-Y. Chui, M. F. Y. Ng, C.-M. Che, *Chem. Eur. J.* **2005**, *11*, 1739-1749.

[19] a) P. J. Bonasi, D. E. Gindelberger, J. Arnold, *Inorg. Chem.* **1993**, *32*, 5126-5131; b) W. Wojnowski, B. Becker, J. Sabmannshausen, E.-M. Peters, K. Peters, H. G. von Schnering, *Z. Anorg. Allg. Chem.* **1994**, *620,* 1417-1421; c) Y. Takino, K. Tsuge, A. Igashira-Kamiyama, T. Kawamoto, T. Konno, *Chem. Asian J.* **2011**, *6*, 2931-2935.

[20] a) H. Gröenbeck, M. Walter, H. Häkkinen, *J. Am. Chem. Soc.* **2006**, *128*, 10268-10275; b) N. Shao, Y. Pei, Y. Gao, X. C. Zeng, *J. Phys. Chem. A.* **2009**, *113*, 629-632; c) K. A. Kacprzak, O. Lopez-Acevedo, H. Häkkinen, H. Grönbeck, *J. Phys. Chem. C* **2010**, *114*, 13571-13576; d) B. M. Barngrover, C. M. Aikens, *J. Phys. Chem. A* **2011**, *115*, 11818-11823.

[21] K. Morokuma, *J. Chem. Phys.* **1971**, *55*, 1236-1244.

[22] T. Ziegler, A. Rauk, *Theor. Chim. Acta* **1977**, *46*, 1-10.

Entry for the Table of Contents

RESEARCH ARTICLE

Ring-in-ring ↔ [2]catenane interconversion. A ring-in-ring structure of Au(I)-thiolate cluster $[Au(SR)]_{12}$ featuring inter-ring closed-shell metallophilic interactions is formed from [2]catenane $[Au(SR)]_{10}$ in hexane and transforms back to the [2]catenane upon dissolving in CH_2Cl_2 or $CHCl_3$. Spectroscopic measurements and DFT calculations provide useful mechanistic insights.

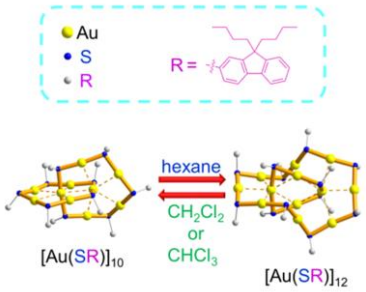

Guang-Tao Xu, Liang-Liang Wu, Xiao-Yong Chang, Tim Wai Hung Ang, Wai-Yeung Wong, Jie-Sheng Huang, Chi-Ming Che**

Page No. – Page No.

Solvent-Induced Cluster-to-Cluster Transformation of Homoleptic Gold(I) Thiolates: between Catenane and Ring-in-Ring Structures